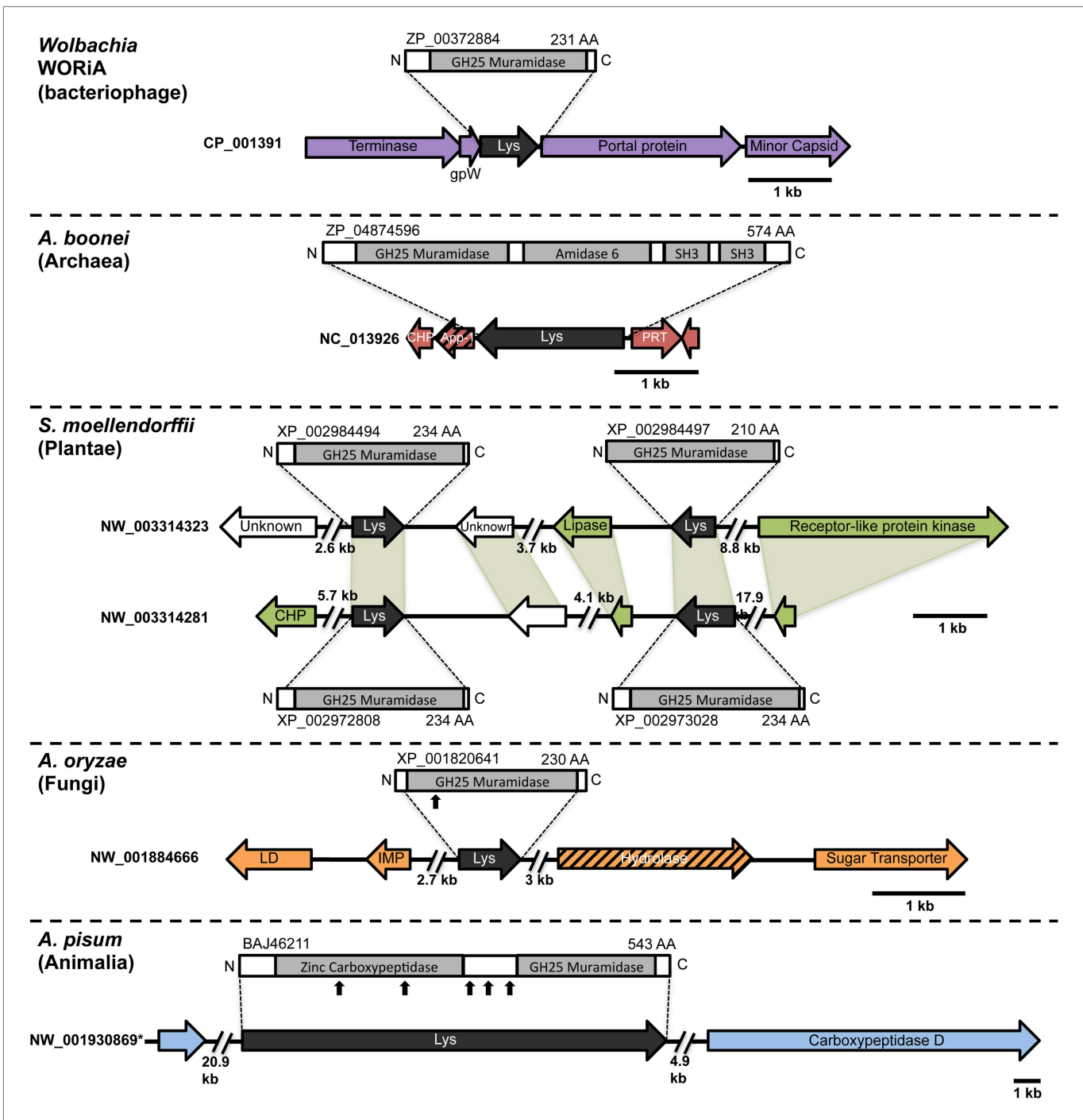


---

## Figures and figure supplements

Antibacterial gene transfer across the tree of life

**Jason A Metcalf, et al.**



**Figure 1.** Architecture of HGT candidates and surrounding genes. Each arrow represents an open reading frame transcribed from either the plus strand (arrow pointing right) or the minus strand (arrow pointing left). The color of the arrow indicates the taxa the gene is found in based on its closest homologs. Black = Eubacteria, purple = virus, red = Archaea, green = Plantae, Orange = Fungi, Blue = Insecta, white = no known homologs, dashed line = present in multiple domains. The length of the arrows and intergenic regions are drawn to scale except where indicated with broken lines. The four paralogs of the lysozyme in *S. moellendorffii* occur on two genomic scaffolds with light green bands connecting homologous genes. Vertical arrows indicate the location of introns in the *A. oryzae* and *A. pisum* lysozymes. Abbreviations: Lys: lysozyme, gpW = phage baseplate assembly protein W, SH3: Src homology domain 3, App-1 = ADP-ribose-1"-monophosphatase, PRT = phosphoribosyltransferase, LD = leucoanthocyanidin dioxygenase; IMP = integral membrane protein. A protein diagram for each lysozyme is drawn to scale with the light gray regions highlighting a conserved protein domain. \**A. pisum* diagram is based on Acyr\_1.0 assembly and transcription data (Nikoh et al., 2010); the annotation in Acyr\_2.0 is different. DOI: 10.7554/eLife.04266.003

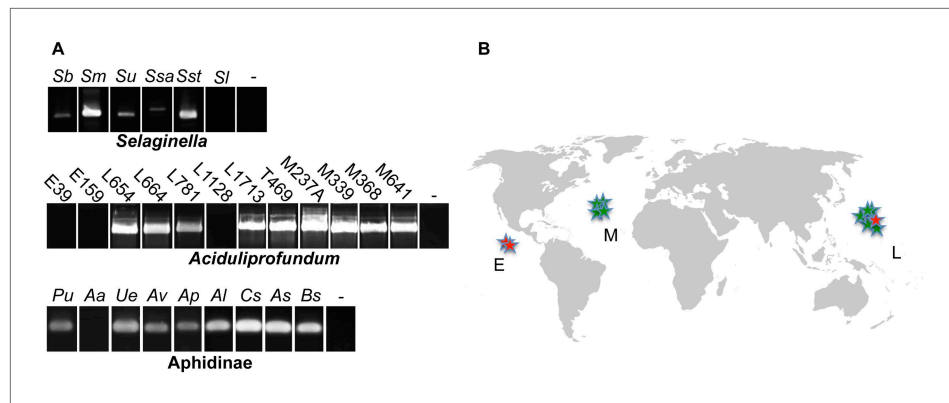


**Figure 1—figure supplement 1.** Presence of HGT lysozyme genes in field samples. **(A)** PCR amplifications of portions of the GH25 muramidase domain in the indicated taxa. All amplifications were Sanger sequenced to confirm integration. Primers used are listed in Table S3. Abbreviations: Sb: *S. braunii*, Sm: *S. moellendorffii*, Su: *S. uncinata*, Ssa: *S. sanguinolenta*, Sst: *S. stauntoniana*, Sl: *S. lepidophylla*, E: East Pacific Rise, L: Lao Spreading Center, M: Mid-Atlantic Ridge, Pu: *Pleotrichophorus utensis*, Aa: *Artemisaphis artemisicola*, Ue: *Uroleucon erigeronensis*, Av: *Aphis varians*, Ap: *Acyrtosiphon pisum*, Al: *Aphis lupini*, Cs: *Cedoaphis* sp., As: *Aphthargelia symphoricarpi*, Bs: *Braggia* sp., - denotes water only control. **(B)** World map with approximate locations of *A. boonei* field samples. Those that tested positive for the GH25 muramidase domain are indicated by green stars and those that tested negative are indicated by red stars. Map is a public domain image from Wikimedia Commons.

DOI: 10.7554/eLife.04266.004

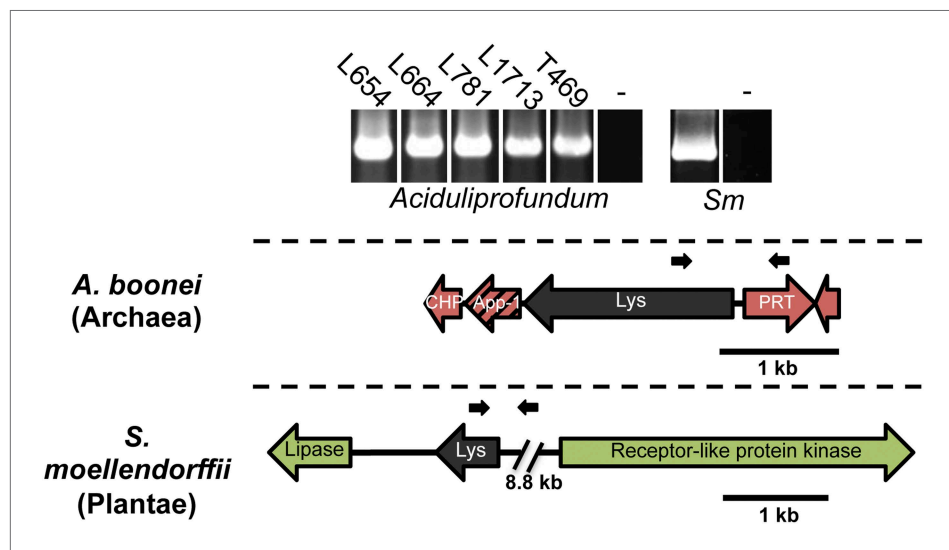


**Figure 1—figure supplement 2.** PCR amplifications testing genomic integration with primers within and outside of lysozyme genes. Primers used are listed in **Supplementary file 1** and binding sites are indicated in gene diagrams with small black arrows. All integrations were confirmed with Sanger sequencing. Abbreviations: Sm: *S. moellendorffii*, L: Lao Spreading Center, - denotes water only control, CHP = conserved hypothetical protein, App-1 = ADP-ribose-1"monophosphatase, PRT = phosphoribosyltransferase.

DOI: 10.7554/eLife.04266.005

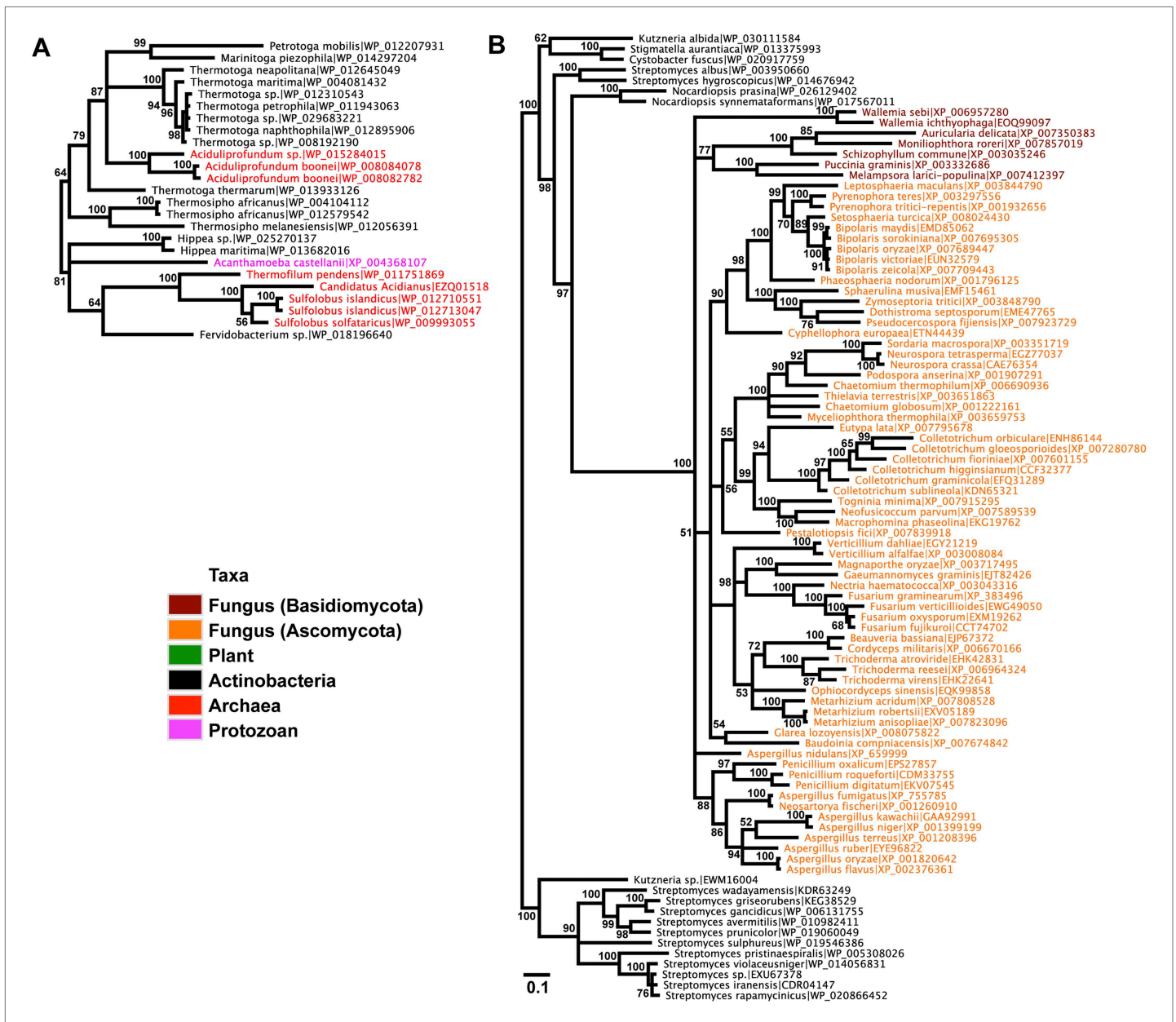


**Figure 1—figure supplement 3.** Protein phylogeny of neighboring genes to transferred lysozymes. (A) App-1 phylogeny based on alignment of 141aa without indels consisting of top E-value hits to blastp using *A. boonei* App-1 as the query. Taxon of origin for each amino acid sequence is indicated by color. Posterior probability is indicated at all nodes with values above 50. Branch lengths represent number of substitutions per site as indicated by scale bar. Tree is arbitrarily rooted. (B) GH2 hydrolase phylogeny based on an alignment of 188aa without indels consisting of top E-value hits to blastp using *A. oryzae* hydrolase as the query.

DOI: [10.7554/eLife.04266.006](https://doi.org/10.7554/eLife.04266.006)

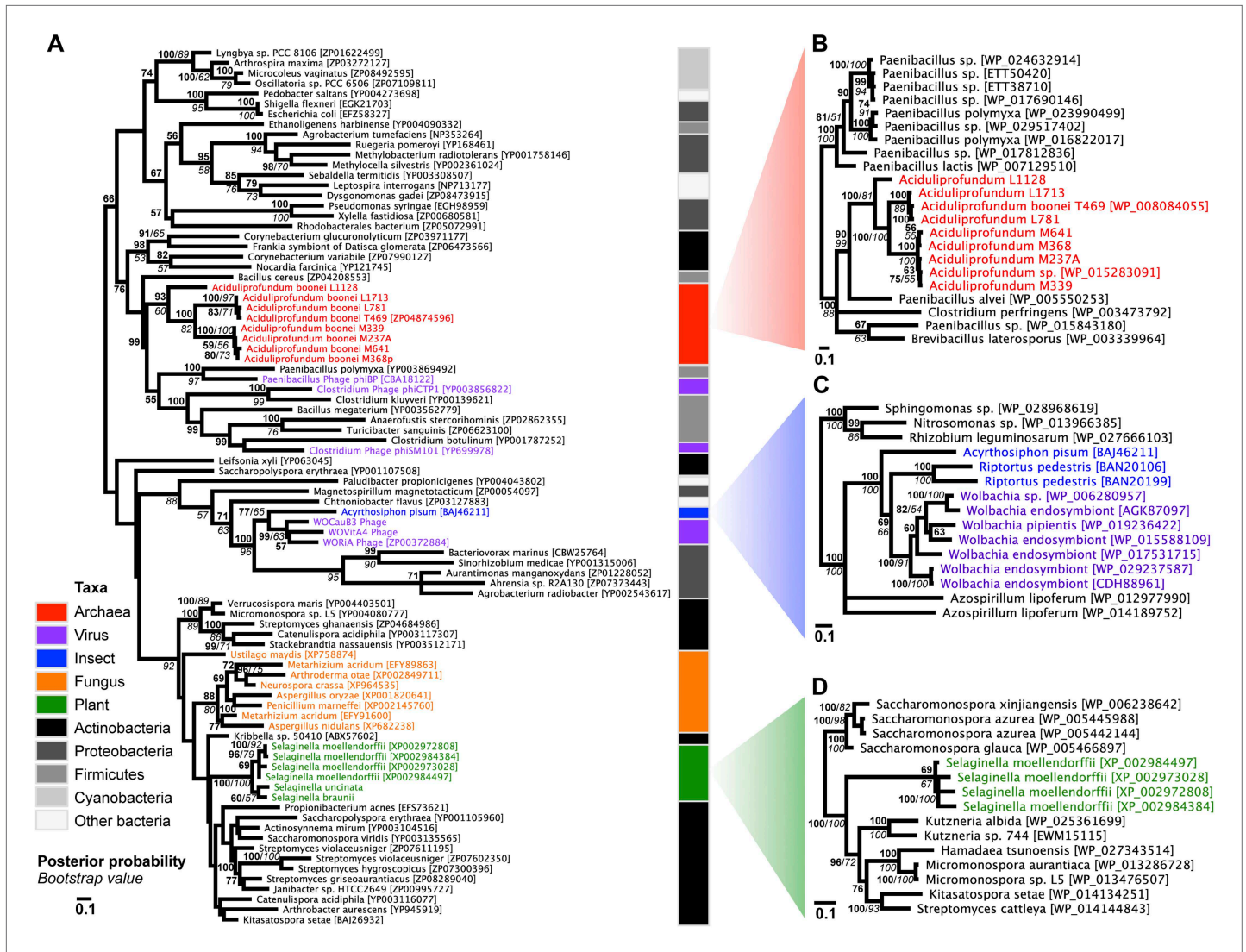


**Figure 2.** Phylogeny of GH25 muramidase. **(A)** Phylogeny based on alignment of 113aa without indels consisting of top E-value hits to blastp using WORiA phage lysozyme as a query. Taxon of origin for each amino acid sequence is indicated by color. Posterior probability (Bayesian phylogeny) and bootstrap values (maximum likelihood phylogeny) are indicated at all nodes with values above 50. Branch lengths represent number of substitutions per site as indicated by scale bar. Tree is arbitrarily rooted. Iterative phylogenies based on top E-value blastp hits to *A. boonei* lysozyme **(B)**, *A. pisum* lysozyme **(C)**, and *S. moellendorffii* lysozyme **(D)** are also shown.

DOI: 10.7554/eLife.04266.007

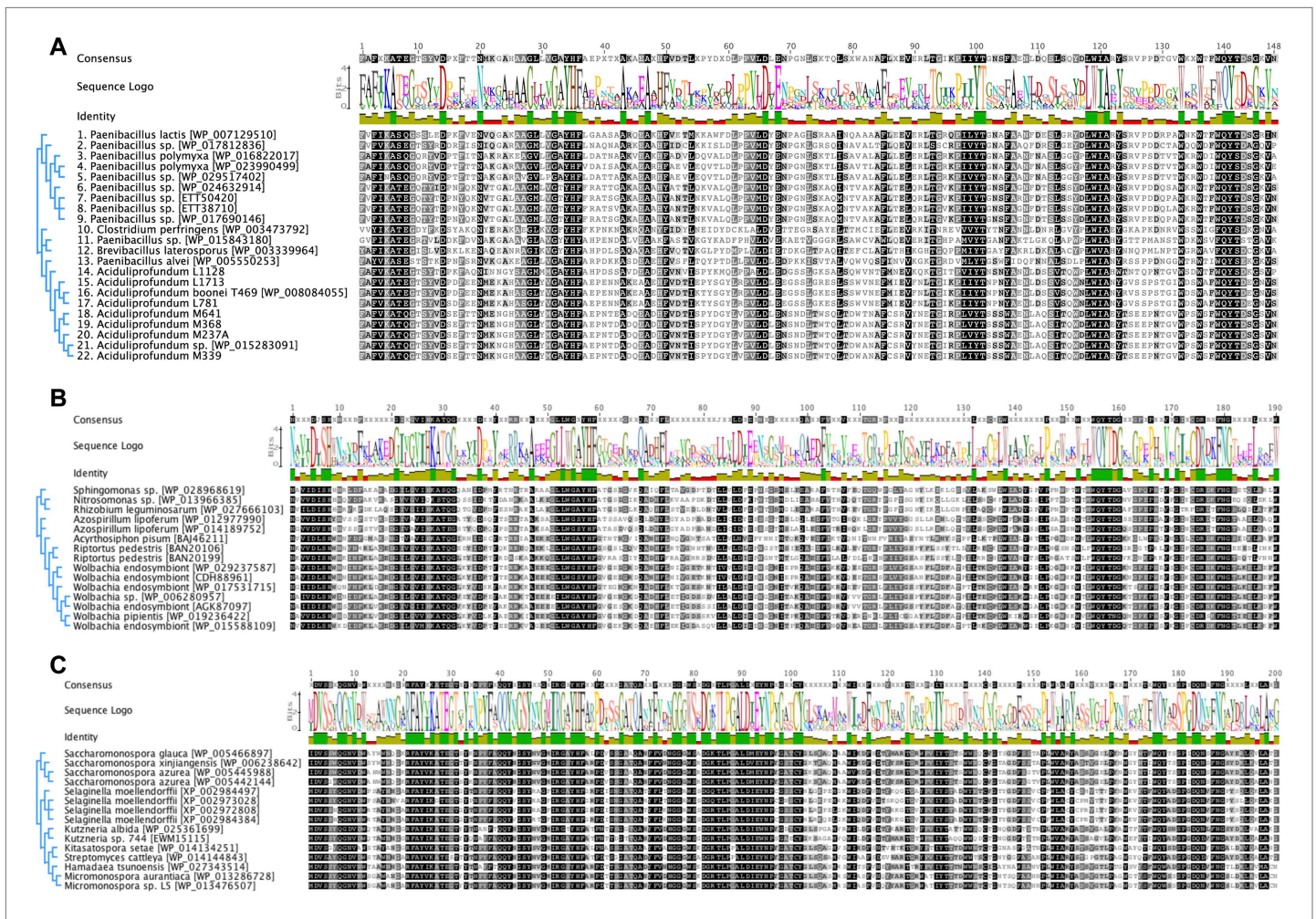


**Figure 2—figure supplement 1.** Iterative HGT analysis alignments. Consensus alignment of GH25 muramidases without indels used in iterative phylogenies in **Figure 2** is shown for **(A)** *A. boonei*, **(B)** *A. pisum*, and **(C)** *S. moellendorffii*. Conservation is indicated by amino acid symbol size and bar graphs below the consensus sequence.

DOI: 10.7554/eLife.04266.008

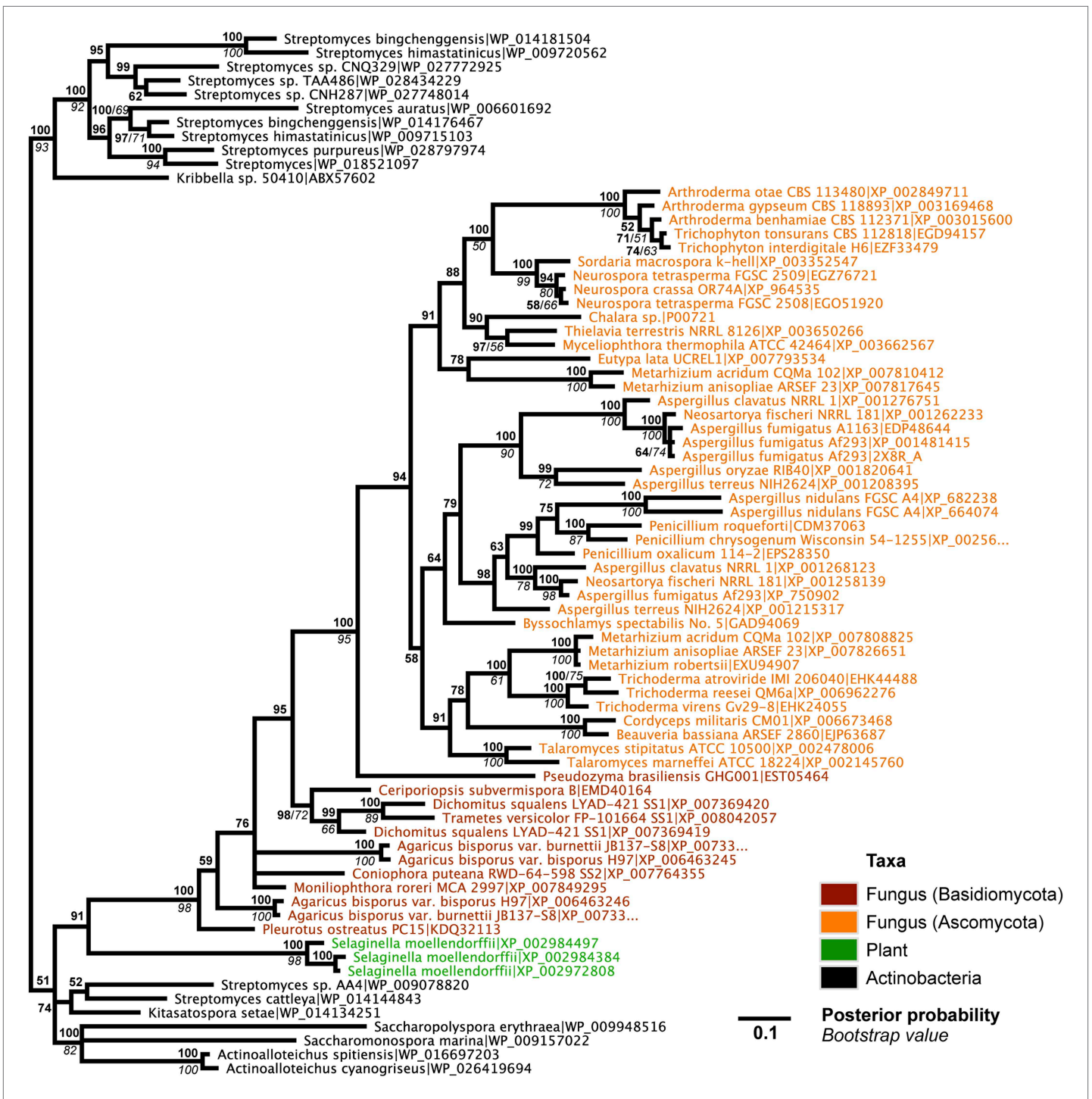


**Figure 2—figure supplement 2.** Protein phylogeny of *A. oryzae* GH25 muramidase and relatives. Phylogeny based on alignment of 186aa without indels consisting of top E-value hits to blastp using *A. oryzae* lysozyme as a query. Taxon of origin for each amino acid sequence is indicated by color. Posterior probability (Bayesian phylogeny) and bootstrap values (maximum likelihood phylogeny) are indicated at all nodes with values above 50. Branch lengths represent number of substitutions per site as indicated by scale bar. Tree is arbitrarily rooted.

DOI: [10.7554/eLife.04266.009](https://doi.org/10.7554/eLife.04266.009)

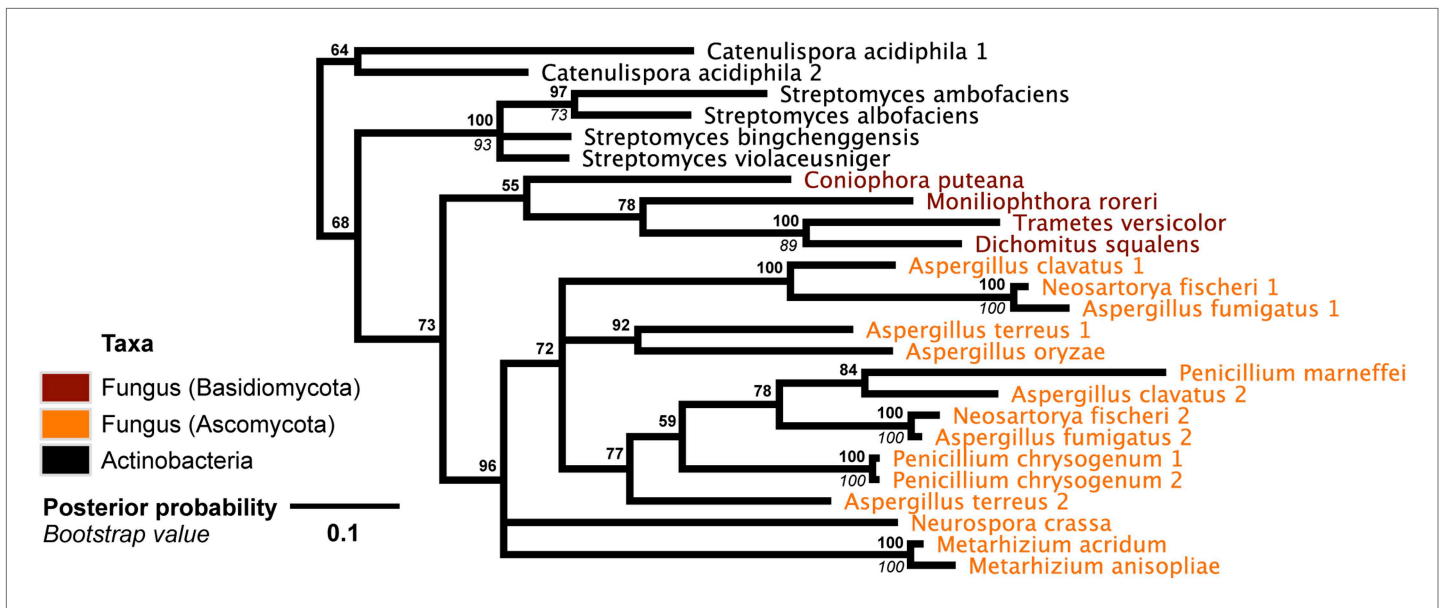


**Figure 2—figure supplement 3.** DNA phylogeny of *A. oryzae* GH25 muramidase and relatives. Phylogeny based on alignment of 282 bp without indels consisting of top E-value hits to blastn using *A. oryzae* lysozyme exon 2 as a query. Taxon of origin for each nucleic acid sequence is indicated by color. Posterior probability (Bayesian phylogeny) and bootstrap values (maximum likelihood phylogeny) are indicated at all nodes with values above 50. Branch lengths represent number of substitutions per site as indicated by scale bar. Tree is arbitrarily rooted.

DOI: [10.7554/eLife.04266.010](https://doi.org/10.7554/eLife.04266.010)

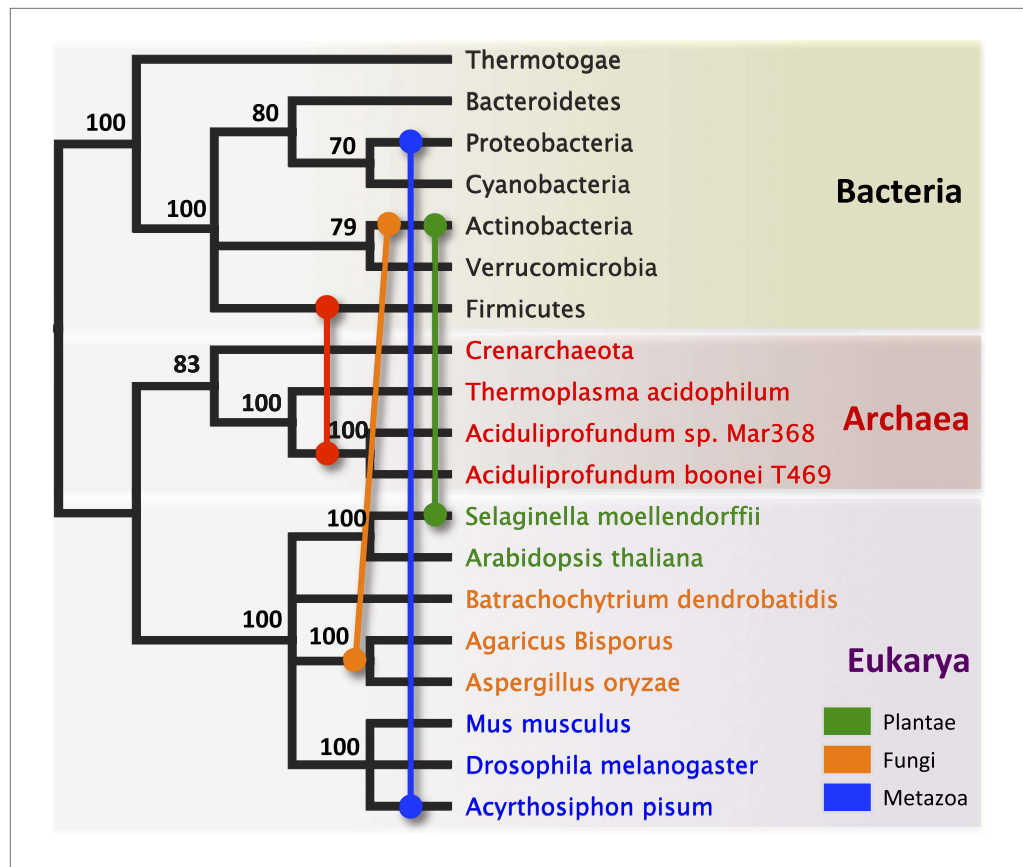


**Figure 3.** Schematic of HGT events. Bayesian phylogeny based on the 16S rRNA gene from selected taxa is shown. Colored lines indicate putative horizontal gene transfer events, although other possible HGT patterns cannot be definitively excluded. Posterior probabilities are noted at each node.  
 DOI: [10.7554/eLife.04266.011](https://doi.org/10.7554/eLife.04266.011)

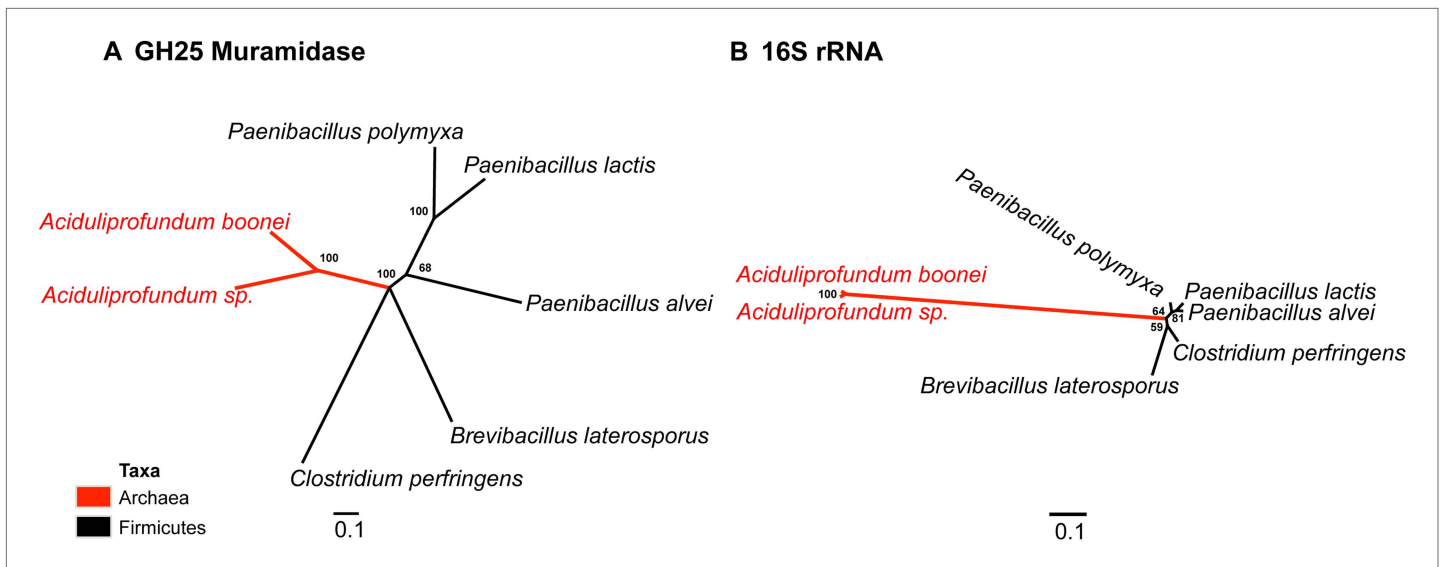


**Figure 4.** Comparison of GH25 muramidase and rRNA divergence. **(A)** Unrooted Bayesian phylogeny of the GH25 muramidase from *A. boonei* and selected relatives, based on an alignment of 185aa without indels. Taxon of origin for each nucleic acid sequence is indicated by color. Posterior probability is indicated at all nodes with values above 50. Branch lengths represent number of substitutions per site as indicated by scale bar. **(B)** Unrooted Bayesian phylogeny of the 16S rRNA gene for the same taxa as in **(A)**, based on an alignment of 1,156 bp without indels. DOI: 10.7554/eLife.04266.012

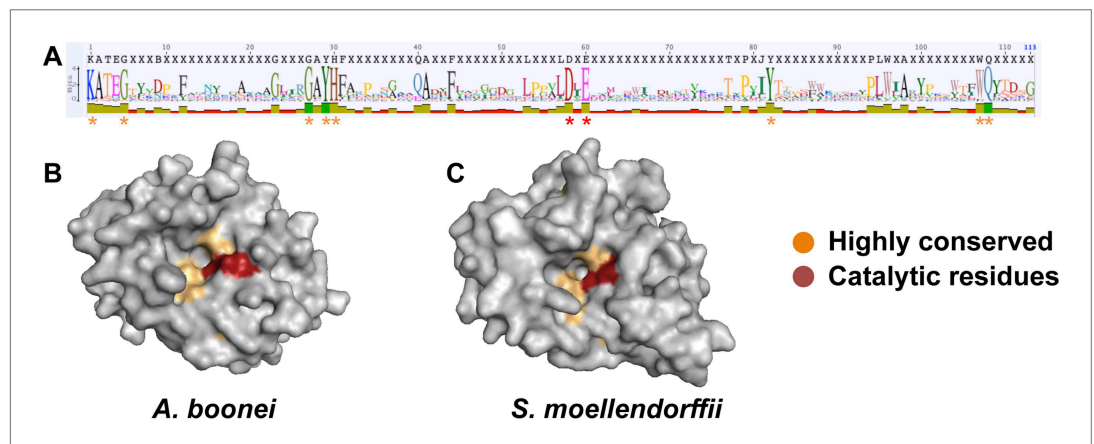


**Figure 5.** Conservation of *A. boonei* GH25 muramidase domain. **(A)** Consensus alignment of 86 GH25 muramidases with insertions and deletions removed. Conservation is indicated by amino acid symbol size and bar graphs below the consensus sequence. Active site residues and highly conserved amino acids modeled below are indicated with red and orange asterisks, respectively. **(B)** Space-filling model of the active site face of the predicted structure of *A. boonei* GH25 muramidase domain and **(C)** *S. moellendorffii* GH25 muramidase domain. Active site residues are indicated in red and the eight additional residues most highly conserved across all 86 proteins are orange.

DOI: 10.7554/eLife.04266.013

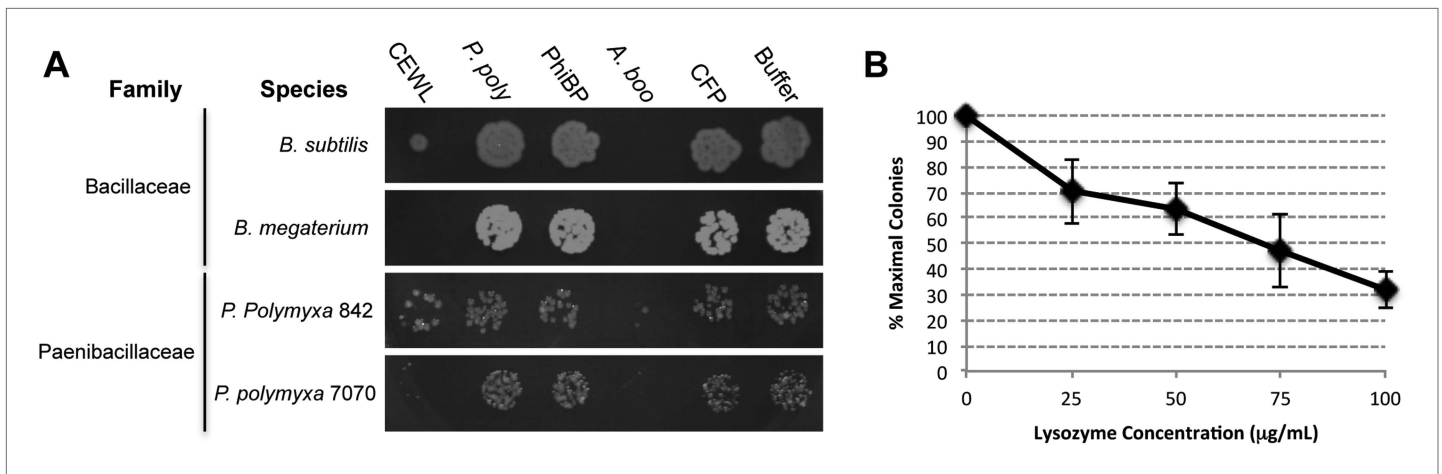


**Figure 6.** Antibacterial action of *A. boonei* GH25 muramidase domain against Firmicutes. **(A)** Bacteria of the specified strain/species incubated overnight on tryptic soy agar after a 20-min liquid preincubation with the proteins indicated. Genera: *B* = *Bacillus*, *P* = *Paenibacillus*. Proteins: CEWL = chicken egg white lysozyme, *P. poly* = *P. polymyxa* lysozyme, PhiBP = bacteriophage PhiBP lysozyme, *A. boo* = GH25 domain of *A. boonei* lysozyme, CFP = cyan fluorescent protein. Images are representative of at least three independent experiments. **(B)** Dose-dependence of *A. boonei* GH25 muramidase antibacterial action. *B. subtilis* colony survival is shown after incubation with *A. boonei* GH25 muramidase at the indicated concentrations for 20 min at 37°C. N = 10 for each concentration.  $p < 0.001$  for linear model fit. Error bars are  $\pm$  SEM.

DOI: 10.7554/eLife.04266.014

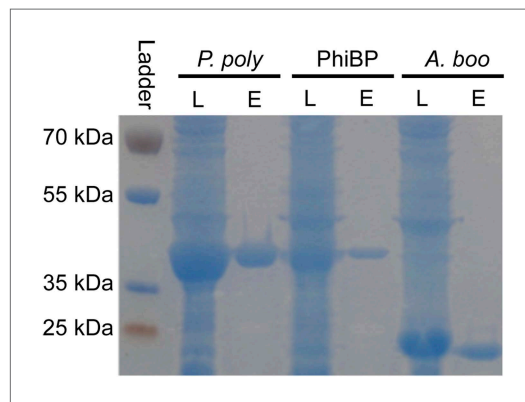


**Figure 6—figure supplement 1.** Lysozyme purifications. PAGE gel stained with GelCode blue before and after purification of 6x-histidine tagged enzymes using nickel affinity chromatography. L = crude *E. coli* lysate expressing the indicated lysozyme, E = elution after lysozyme purification. *P. poly* = *P. polymyxa* lysozyme, PhiBP = bacteriophage PhiBP lysozyme, *A. boo* = *A. boonei* GH25 domain.

DOI: 10.7554/eLife.04266.015

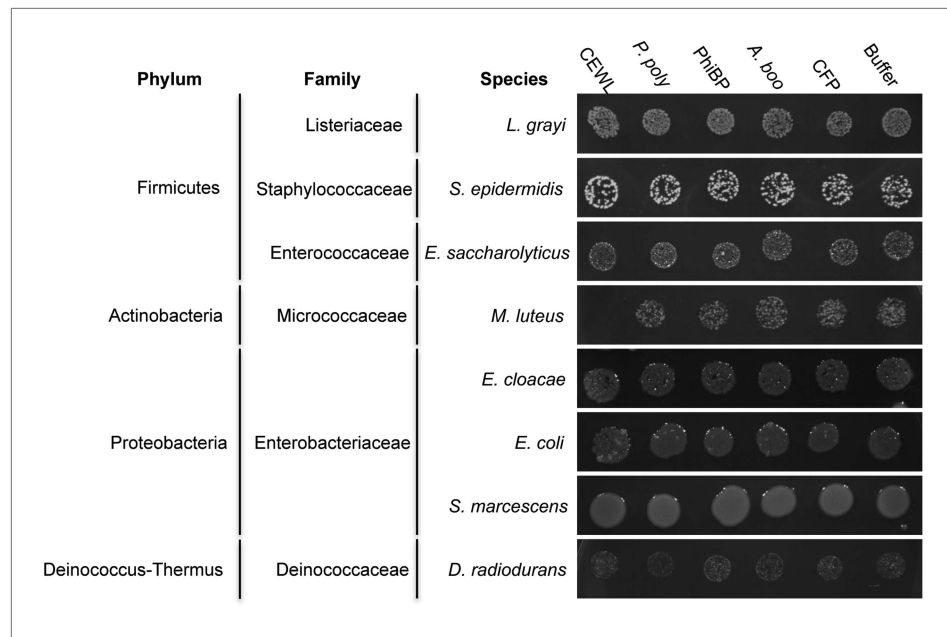


**Figure 6—figure supplement 2.** Antibacterial test of *A. boonei* GH25 muramidase on non-Firmicutes bacteria. Bacteria of the specified strain/species incubated overnight on tryptic soy agar after a 20-min liquid preincubation with the proteins indicated. Genera: L = *Listeria*, S = *Staphylococcus*, E. *saccharolyticus* = *Enterococcus*, M = *Micrococcus*, E. *cloacae* = *Enterobacter*, E. *coli* = *Escherichia*, S = *Serratia*, D = *Deinococcus*. Proteins: CEWL = chicken egg white lysozyme, P. *poly* = *P. polymyxa* lysozyme, PhiBP = bacteriophage PhiBP lysozyme, A. *boo* = GH25 domain of *A. boonei* lysozyme, CFP = cyan fluorescent protein. Images are representative of at least three independent experiments. DOI: 10.7554/eLife.04266.016

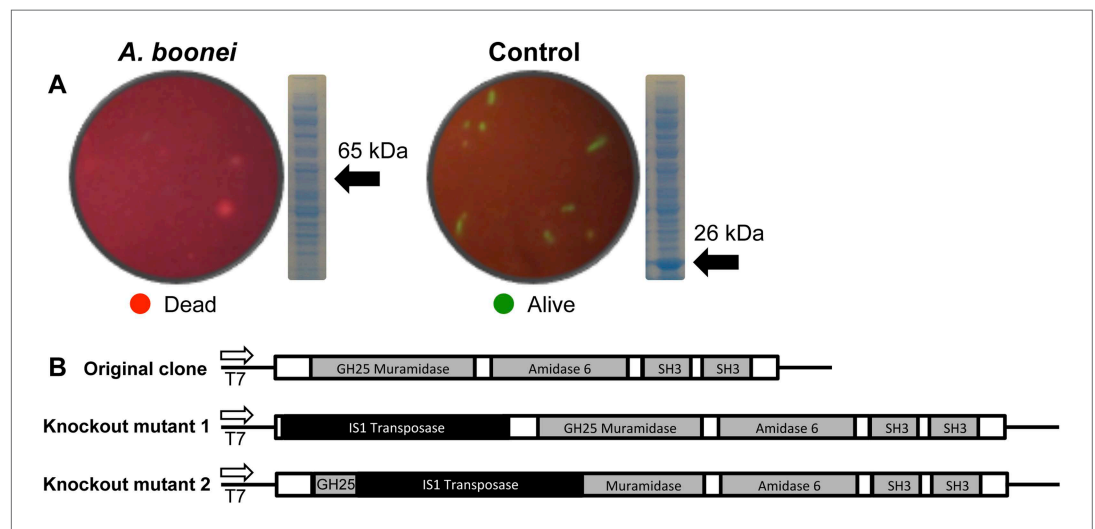


**Figure 7.** *E. coli* death following full-length *A. boonei* lysozyme expression. (A) Live/dead stain of BL21 (DE3) *E. coli* transformed with expression constructs for the full-length lysozyme from *A. boonei* or a control lysozyme WORiA, a bacteriophage infecting *Wolbachia pipientis* strain wRi, after overnight growth without induction. PAGE gels of crude *E. coli* lysates from *E. coli* expressing the indicated lysozyme after 6 hr of induction are also shown with the expected sizes of lysozymes indicated with arrows. (B) Structure of original full-length *A. boonei* lysozyme expression plasmid and two spontaneous knockout mutants caused by insertion of 774 bp (mutant 1) and 768 bp (mutant 2) of IS1 transposase sequences. These insertions also resulted in a number of stop codons in the reading frame of the lysozyme. Knockout mutants grew to normal colony size, while all wild type colonies had intact expression plasmids, grew poorly, and died over time in liquid culture. DOI: 10.7554/eLife.04266.017

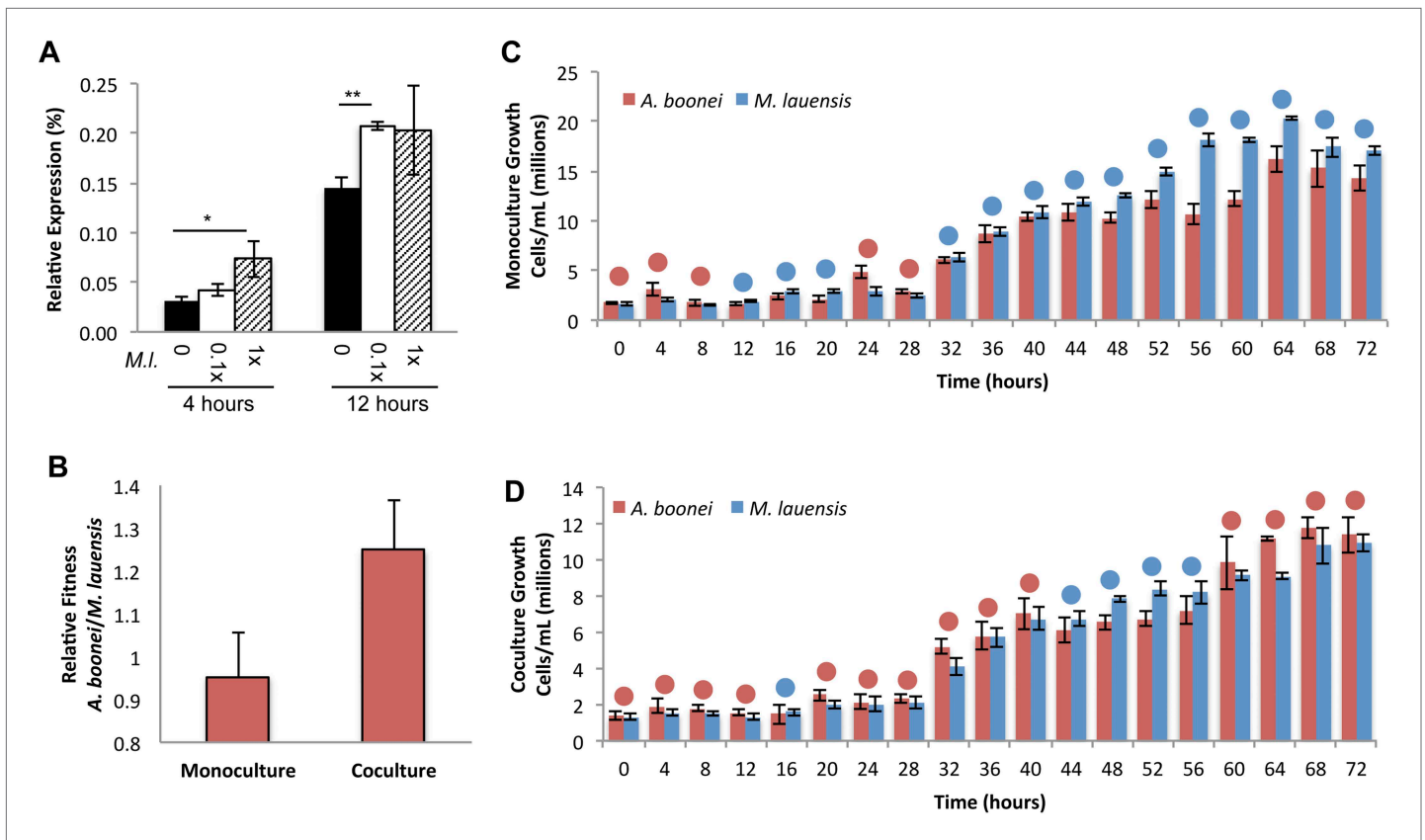


**Figure 8.** Lysozyme expression and relative fitness during *A. boonei* and *M. lauensis* coculture. **(A)** Expression of *A. boonei* GH25 muramidase relative to the control gene elongation factor 1 $\alpha$ , after the indicated time of coculture with *M. lauensis* (*M.l.*) at the specified ratio relative to *A. boonei*. \* $p < 0.05$ , \*\* $p < 0.01$ , by Mann–Whitney U pairwise comparisons.  $N = 6$  for all samples. Primers are listed in **Supplementary file 1**. **(B)** Relative fitness of *A. boonei* vs *M. lauensis* in monoculture ( $N = 5$ ) and coculture ( $N = 4$ ). **(C)** Growth of *A. boonei* (red) and *M. lauensis* (blue) monocultures over time. Significant differences in cell abundance occur at 24, 52, and 64 hr ( $p < 0.05$ ), and 56 and 60 hr ( $p < 0.01$ ) based on pairwise Wilcoxon tests. **(D)** Growth of *A. boonei* and *M. lauensis* in coculture over time. Significant differences in cell abundance occur at 48, 52, and 64 hr ( $p < 0.05$ ) based on pairwise Wilcoxon tests. Error bars are  $\pm$ SEM for all panels.

DOI: [10.7554/eLife.04266.018](https://doi.org/10.7554/eLife.04266.018)